The role of cysteine and sulfide in the interplay between microbial Hg(II) uptake and sulfur metabolism

Journal:	*Metallomics*
Manuscript ID	MT-ART-04-2019-000077.R2
Article Type:	Paper
Date Submitted by the Author:	16-May-2019
Complete List of Authors:	Thomas, Sara; Northwestern University, Civil and Environmental Engineering Catty, Patrice; Laboratoire de Chimie et Biologie des Métaux Hazemann, Jean-Louis; Insitut Néel, CNRS, Michaud-Soret, Isabelle; Laboratoire de Chimie et Biologie des Metaux, Gaillard, Jean-Francois; Northwestern University, Civil and Environmental Engineering

SCHOLARONE™
Manuscripts

Significance to Metallomics

The present study describes how the cellular sulfur metabolism can influence Hg(II) biouptake by bacteria, potentially leading to the misinterpretation of results if not considered. We demonstrate that the high Hg(II) bioavailability previously observed in the presence of excess cysteine is dependent on the biodegradation of cysteine to sulfide and the formation of cell-associated Hg(II)-sulfide species.

1
2
3
4
5
6
7
8
9
10
11
12
13
14
15
16
17
18
19
20
21
22
23
24
25
26
27
28
29
30
31
32
33
34
35
36
37
38
39
40
41
42
43
44
45
46
47
48
49
50
51
52
53
54
55
56
57
58
59
60

The role of cysteine and sulfide in the interplay between microbial Hg(II) uptake and sulfur metabolism

Sara A. Thomas,[1,2]*+ Patrice Catty,[2] Jean-Louis Hazemann,[3] Isabelle Michaud-Soret,[2]* and Jean-François Gaillard[1]*

[1] Department of Civil and Environmental Engineering, Northwestern University, 2145 Sheridan Road, Evanston, IL 60208

[2] Université Grenoble Alpes, CNRS, CEA, BIG-LCBM, 38000 Grenoble, France

[3] Institut Néel, UPR 2940 CNRS—Université Grenoble Alpes, F-38000 Grenoble, France

*Corresponding authors:

Sara A. Thomas

Email: st18@princeton.edu

Phone: +1 (609)-258-2339

1
2
3
4
5   Isabelle Michaud-Soret
6
7   Email: isabelle.michaud-soret@cea.fr
8
9   Phone: +33 4 38 78 99 40
10
11
12   Jean-François Gaillard
13
14   Email: jf-gaillard@northwestern.edu
15
16   Phone: +1 (847)-467-1376
17
18
19
20
21
22
23   + Present address: Department of Geosciences, Princeton University, Guyot Hall, Princeton, NJ 08544
24
25
26
27
28
29
30
31
32
33
34
35
36
37
38
39
40
41
42
43
44
45
46
47
48
49
50
51
52
53
54
55
56
57
58
59
60

1   **Abstract**

2   Biogenic thiols, such as cysteine, have been used to control the speciation of Hg(II) in bacterial exposure

3   experiments. However, the extracellular biodegradation of excess cysteine leads to the formation of

4   Hg(II)-sulfide species, convoluting the interpretation of Hg(II) uptake results. Herein, we test the

5   hypothesis that Hg(II)-sulfide species formation is a critical step during bacterial Hg(II) uptake in the

6   presence of excess cysteine. An *Escherichia coli* (*E. coli*) wild-type and mutant strain lacking the *decR*

7   gene that regulates cysteine degradation to sulfide were exposed to 50 and 500 nM Hg with 0 to 2 mM

8   cysteine. The *decR* mutant released ~4 times less sulfide from cysteine degradation compared to the wild-

9   type for all tested cysteine concentrations during a 3 hour exposure period. We show with thermodynamic

10   calculations that the predicted concentration of Hg(II)-cysteine species remaining in the exposure medium

11   (as opposed to forming $HgS_{(s)}$) is a good proxy for the measured concentration of dissolved Hg(II) (i.e.,

12   not cell-bound). Likewise, the measured cell-bound Hg(II) correlates with thermodynamic calculations

13   for $HgS_{(s)}$ formation in the presence of cysteine. High resolution x-ray absorption near edge structure

14   (HR-XANES) spectra confirm the existence of cell-associated $HgS_{(s)}$ at 500 nM total Hg and suggest the

15   formation of Hg-S clusters at 50 nM total Hg. Our results indicate that a speciation change to Hg(II)-

16   sulfide controls Hg(II) cell-association in the presence of excess cysteine.

17

18

19

20

21

22   **Introduction**

23   The bioaccumulation of alkylated mercury (Hg) species poses significant risks to ecosystem and human

24   health. However, the mechanism of bacterial uptake of inorganic Hg(II) species that leads to alkyl-

25   mercury (e.g., methylmercury – MeHg) formation remains unknown.[1] One way to gain insight into the

26   uptake mechanism, which has been extensively investigated in the literature, is to test how the Hg(II)

27   speciation in the exposure medium can affect Hg(II) bioavailability.[2-12] In the environment, Hg(II) is

28   expected to be bound to either thiol groups of low molecular weight ligands/natural organic matter

29   (NOM) or sulfides due to the high affinity of Hg(II) for reduced sulfur.[13] Among various thiols,

30   exogenous cysteine has been shown to play an important role in regulating Hg(II) uptake, greatly

31   enhancing or inhibiting it depending on the cysteine and Hg(II) concentration.[3-5, 7, 11, 14, 15]

32   Cysteine is an amino acid that plays a central role in cellular sulfur metabolism.[16, 17] A few of the

33   various metabolic pathways involving cysteine include the biosynthesis of methionine, the formation of

34   iron sulfur (Fe-S) clusters, and the biosynthesis of glutathione.[16, 18-24] The thiol group of cysteine assists

35   protein folding via the formation of disulfide bonds, exists in the catalytic sites of enzymes, and binds

36   strongly to soft acid metals (e.g., Hg(II), Cd(II), Pb(II), and Ag(I)).[24] However, due to its high reactivity,

37   cysteine is toxic to cells. As a result, cells have complex regulatory systems to maintain strict control of

38   intracellular cysteine concentrations.[17] In response to increased intracellular cysteine concentration,

39   cysteine desulfhydrase and/or desulfidase enzymes are activated to degrade cysteine into hydrogen

40   sulfide, pyruvate, and ammonium.[25-29] Although the biodegradation of biologically important thiols (e.g.,

41   cysteine and glutathione) has been well documented,[30-32] past Hg(II) uptake experiments have rarely

42   considered how the Hg(II) speciation in the exposure medium may change over time due to ligand

43   degradation or secretion by the bacteria. The ability of exogenous thiols to degrade into sulfide and the

44   ability of bacteria to produce sulfide endogenously (i.e., not limited to dissimilatory sulfate reduction) is

45   of particular importance for understanding Hg(II) bioavailability because previous studies have reported

46   that neutral Hg(II)-sulfide species are bioavailable to bacteria via passive diffusion.[10, 33, 34]

4

47   Previous studies, including our own, have shown, relying on thermodynamic calculations, that the

48   sulfide released from exogenous cysteine degradation can outcompete excess cysteine and bind Hg(II) in

49   the exposure medium.[10, 12, 35, 36] In agreement with these calculations, we have shown using x-ray

50   absorption spectroscopy (XAS) and scanning transmission electron microscopy (STEM) that cell-

51   associated $HgS_{(s)}$ nanoparticles form after the exposure of *Escherichia coli*, *Geobacter sulfurreducens*,

52   and *Bacillus subtilis* to Hg(II) and excess cysteine.[35] Pre-equilibrated Hg(II)-cysteine complexes that are

53   added to cell suspensions will form cell-associated $\alpha\text{-}HgS_{(s)}$ or $\beta\text{-}HgS_{(s)}$ at relatively high total added

54   Hg(II) concentrations (500 nM – 5 µM) and short time scales (< 1 hour). At lower added Hg(II)

55   concentrations (50 nM), we also observed the formation of cell-associated Hg(II)-sulfide species from

56   Hg(II)-cysteine complexes. However, the relatively low signal to noise ratio of conventional XAS at these

57   Hg(II) concentrations limited our ability to determine the nature of the Hg(II)-sulfides (e.g.,

58   nanoparticulate $\beta\text{-}HgS_{(s)}$ or smaller, β-HgS-like Hg-S clusters). In addition, we were unable to directly

59   relate Hg(II)-sulfide species formation to Hg(II) uptake into the cytoplasm.

60   The goal of this study is to further investigate Hg(II) bioavailability by testing the hypothesis that

61   when sulfide and cysteine coexist in the exposure medium, Hg(II)-sulfide species, and not Hg(II)-cysteine

62   species, undergo biouptake. Due to the simplicity of modifying the genome, wild-type and mutant strains

63   of *E. coli* lacking single genes involved in sulfide biosynthesis (Δ*decR*, Δ*sufS*, and Δ*iscS*) were chosen for

64   these experiments. We exposed bacterial cells to 50 or 500 nM total Hg(II) that was pre-equilibrated with

65   0 to 2 mM cysteine so that Hg(II) was introduced to exposure assays as Hg(II)-cysteine complexes with

66   an excess of cysteine. Over a period of 3 hours, we quantified the total cysteine, total sulfide, and total Hg

67   concentration in the exposure medium every hour in order to predict Hg(II) speciation. To identify the

68   cell-associated Hg(II) coordination environment, we probed cell pellets that were exposed to Hg(II) ±

69   cysteine for 3 hours with high energy resolution X-ray absorption near edge structure (HR-XANES)

70   spectroscopy.

71   **Materials and methods**

72   ***Bacterial strains***

73   Keio collection strains of *E. coli* single-gene deletion mutant JW0437 (Δ*decR*, formerly known as Δ*ybaO*)

74   as well as wild-type *E. coli* K-12 (BW25113) were obtained from the *E. coli* Genetic Stock Center.[37] The

75   cysteine desulfurase mutants (Δ*iscS* and Δ*sufS*) were obtained from the BioCat team in the Chemistry and

76   Biology of Metals Laboratory (Grenoble, France) and are described in detail in Ranquet et al.[38] The

77   strains were regenerated from sterile filter disks or frozen glycerol stock (stored at -80 ^{o}C) onto LB agar

78   (with 50 mg/L kanamycin for mutants) at 37 ^{o}C for 24 hours. The strains were stored on LB agar plates at

79   4 ^{o}C for no longer than 4 weeks.

80   ***Growth media and cell harvesting***

81   A single colony of *E. coli* from a refrigerated LB agar plate was inoculated into ∼3 mL of LB broth in a

82   sterile, 12 mL polypropylene tube and incubated aerobically at 37 ^{o}C with medium shaking for ∼6 hours.

83   Subsequently, 20 – 100 µL of the cell suspension was inoculated into 50 – 100 mL of minimal salts

84   medium (MSM; Table S1) in sterile, foil-topped 125 mL or 250 mL Erlenmeyer flasks and shaken at 37

85   ^{o}C overnight. Cells were harvested in MSM during exponential growth phase (OD_{600} = 0.2). Cells were

86   washed twice with minimal complexing medium (MCM) – the exposure medium for Hg(II) b024 biouptake

87   assays – and resuspended to a density of 2×10^8 cells/mL, which is equivalent to an OD_{600} of 0.2. MCM

88   is buffered to pH = 7.1 with 20 mM MOPS and contains 1 mM Na-β-glycerophosphate, 0.41 mM $MgSO_4$,

89   12 mM NH_4NO_3, 0.76 mM isoleucine, 0.76 mM leucine, 3 nM thiamine, 10 mM glucose, and 9.1 mM

90    $NaOH$.[8] All mutant strains of *E. coli* were grown in the presence of 50 mg/L kanamycin.

91   ***Hg(II) and cysteine exposure assays***

92   A 10 mM $Hg(NO_3)_2$ stock solution in 1% HNO_3 (trace metal grade; TMG) was used for all exposure

93   assays and stored at 4 ^{o}C. A 100 mM cysteine stock solution was prepared in deionized water (18 MΩ)

94   immediately before use. Hg(II) and cysteine were pre-equilibrated for 1 hour in deionized water (18 MΩ)

95   at 10 times the final desired concentrations (fixed molar ratios of 1:2,000, 1:10,000, 1:20,000, or 1:40,000

96   Hg:Cys) prior to being added to cell suspensions. Hg(II) and cysteine exposure assays were aerobic and

97   conducted in 15 mL borosilicate glass vials or 125 mL Erlenmeyer flasks with 7 mL and 50 mL total

98   volume, respectively. The assays were conducted under dark conditions at 37 $^{\circ}$C and initiated with the

99   addition of Hg(II) solution (± cysteine) to the cell suspension in MCM so that the Hg(II) solution (±

100   cysteine) was diluted by a factor of 10. The pH was measured before and after exposure to Hg(II) ±

101   cysteine in MCM and did not significantly vary from the initial pH of 7.1.

102   *Hg(II)-cell sorption measurements*

103   After cell suspensions mixed with Hg(II) and cysteine for 0, 1, 2, and 3 hours (7 mL total volume), ~700

104   µL aliquots were collected at each time point for the determination of (1) total recoverable Hg (dissolved

105   + cell-bound) and (2) dissolved Hg (after filtration on a 0.2 µm nylon filter, VWR International). As we

106   documented earlier, the nylon filters do not bind a significant amount of Hg.[36] The samples at 0 hours

107   were collected as soon as possible after Hg addition to cell suspensions, and thus, cells were exposed to

108   Hg(II) for up to 1 minute of mixing. The cell-bound Hg was calculated as the difference between the total

109   recoverable Hg and the dissolved Hg. Samples for determining dissolved and total recoverable Hg were

110   preserved in ~1% HCl (TMG) until the measurement of total Hg with a Direct Mercury Analyzer (DMA-

111   80, Milestone).

112   *Sulfide and cysteine detection in the exposure medium*

113   After mixing cells with cysteine for 0, 1, 2, and 3 hours (7 mL total volume), a 1 mL aliquot was

114   centrifuged (15,000 g for 5 min) for the determination of acid labile sulfide in the supernatant by a

115   method adapted from Cline[39, 40] as well as cysteine and cystine (oxidized cysteine) by a method adapted

116   from Gaitonde.[41] Both the Cline and Gaitonde methods are colorimetric and specific to sulfide and

117   cysteine, respectively. Detailed methods are reported in our previous publication.[36] The detection limit for

118   sulfide and cysteine was 2 µM and 5 µM, respectively.

119   *Bacterial samples for HR-XANES measurements*

120 After a 3 hour exposure of cells to Hg(II) ± cysteine (50 mL total volume), the cells were washed 2 times

121 by centrifugation (8,000 g for 5 min) with an equivalent volume of 0.1 M NaClO₄.[42] During the washing

122 steps, the cell suspension was resuspended in smaller volumes in succession until cells were in a 1 mL

123 final suspension of 0.1 M NaClO₄. The 1 mL of suspension was added to a 1.5 mL centrifuge tube

124 containing a 0.2 μm cellulose acetate centrifugal filter (~8 mm diameter cut with a hole punch). The tube

125 was centrifuged briefly for 2 minutes at ~3,000 g so that the cells were collected on the filter and the

126 medium passed through the filter. The filter paper containing pelleted cells was subsequently sandwiched

127 between 2 pieces of Kapton tape and immediately plunged in liquid nitrogen. The samples were stored at

128 -80 °C for no more than 1 week and remained frozen throughout analysis.

129 ***HR-XANES experimental setup and analysis.***

130 The HR-XANES experiments were performed at the European Synchrotron Radiation Facility (ESRF) at

131 beamlines BM30B FAME and BM16 FAME-UHD. All Hg standards and samples were measured in high

132 energy resolution fluorescence detection (HERFD) mode with 5 spherically bent Si(111) crystal analyzers

133 (bending radius = 1 m, crystal diameter = 0.1 m). The Hg $L_{\alpha1}$ fluorescence line (apparent core-hole

134 lifetime broadening of 2.12 eV)[43] was selected using the 555 reflection, and the diffracted fluorescence

135 was measured with a silicon drift detector (SDD, Vortex EX-90). The monochromator was calibrated with

136 a Se reference foil (K-edge = 12,658 eV), and a $HgCl_2$ powder was scanned at the start of each

137 experiment to maintain relative energy calibration. Hg powder standards were finely ground, diluted to

138 ~0.5 wt% with boron nitride, pressed into ~5 mm diameter pellets, and loaded onto a copper sample

139 holder. Liquid Hg reference standards were pipetted into a copper sample holder sealed on two ends with

140 Kapton tape and immediately plunged into LN_2 to minimize contact of the liquid with the copper as well

141 as to prevent the formation of ice during freezing. Frozen bacterial samples were fixed onto copper

142 sample holders with grease and quickly plunged into liquid nitrogen to prevent the sample from thawing.

143 All liquid Hg references and bacterial samples containing Hg were measured at 10 – 15 K. Powdered Hg

144 references (α-HgS$_{(s)}$ and β-HgS$_{(s)}$) were measured at 10 – 15 K and room temperature for comparison.

145 Data normalization and linear combination fits of the XANES to determine the Hg speciation in bacterial

146 samples were performed with Athena.[44] Details on the preparation of Hg reference standards for HR-

147 XANES is provided in the SI (page S2).

Sample preparation and imaging with TEM

149 After mixing cells with Hg(II) ± cysteine for 3 hours, a 1 – 2 mL aliquot was collected and

150 washed 4 times with 0.1 M NaClO$_4$ by centrifugation (8000 g for 3 min) in a 1.5 – 2 mL microfuge tube

151 to remove Hg not associated with cells. After the final wash, the cells were resuspended in a solution of

152 200 μL filtered Milli-Q water (0.2 μm filter, VWR International). One drop (< 5 μL) was immediately

153 placed on a 200 mesh carbon-coated copper grid and allowed to air dry for ~10 minutes. TEM

154 micrographs and selected area electron diffraction (SAED) patterns were collected at room temperature

155 with a Hitachi H-8100 transmission electron microscope using an accelerating voltage of 200 kV.

Thermodynamic calculations

157 The speciation calculations for Hg(II) were performed with the program ChemEQL.[45] The equilibrium

158 constants used in the calculations are reported in Table S2.

Results and Discussion

Sulfide production from cysteine degradation

161 The transcription factor DecR (formerly known as YbaO) activates the *yhaOM* operon, where the *yhaO*

162 gene is predicted to be responsible for cysteine import and the *yhaM* gene appears to have cysteine

163 desulfhydrase (also known as desulfidase) activity.[28] *yha*M is cysteine-inducible and has been shown to

164 have the most significant role in cysteine detoxification in *E. coli* among the numerous other reported

165 enzymes (e.g., TnaA, CysK, CysM, MalY, and MetC).[46] The deletion of the *decR* gene was previously

166 shown to strongly limit the desulfhydrase activity in *E. coli*.[28] We exposed a wild-type and *decR* deletion

167 mutant strain of *E. coli* to cysteine concentrations ranging from 0 to 2 mM and measured the total acid

168   labile sulfide concentration in the exposure medium every hour for 3 hours (Figure 1) by the Cline

169   method.[39]

170   All added cysteine concentrations tested lead to essentially the same sulfide concentration in the

171   exposure medium at each time point for both the wild-type and *decR* mutant, indicating that cysteine

172   degradation to sulfide reaches a threshold for both strains at 0.5 mM added cysteine and above. Notably,

173   the sulfide concentration in the exposure medium reaches a maximum of ~40 µM (2 hours) for the wild-

174   type strain but only ~10 µM (1 – 2 hours) for the *decR* mutant. After just 1 hour of exposure, the

175   measured sulfide concentration in the exposure medium for all added cysteine concentrations is ~20 µM

176   and 5 -10 µM for the wild-type and *decR* mutant, respectively. Although the *decR* mutant is still able to

177   degrade cysteine and release sulfide into the exposure medium, the loss of cysteine desulfhydrase activity

178   results in a significant decrease in the concentration of total sulfide in the exposure medium.

179   The concentrations of reduced and total cysteine (i.e., reduced + oxidized) in the exposure

180   medium have also been quantified under the same conditions as the sulfide measurements (Figure 2) by

181   the Gaitonde method, which is cysteine-specific and not affected by similar thiols (e.g., glutathione and

182   homocysteine).[41] A Tukey's honest significant differences test was performed on the wild-type and *decR*

183   mutant datasets for each added cysteine concentration (i.e., 0.5, 1, and 2 mM) to determine the statistical

184   significance ($p < 0.05$) between the measurements. At $t = 0$ hours, the concentration of reduced cysteine

185   is less than the total cysteine due to the known oxidation of cysteine in the exposure medium.[35, 36] Thus,

186   all assays begin with reduced cysteine concentrations that are ~70 to 90% of the total added cysteine, with

187   cystine accounting for the remainder. With increased incubation time, the cysteine concentration in all

188   assays decreases, mainly due to cysteine biouptake/biodegradation and not oxidation because the total

189   cysteine concentration (reduced + oxidized) also decreases by nearly the same amount. The most notable

190   decrease in cysteine concentration is observed in the wild-type cells exposed to 0.5 mM cysteine, where

191   the initial reduced cysteine concentration drops from ~0.35 mM to ~0.2 mM after 2 hours of exposure.

192   The decrease in the concentration of cysteine is not as drastic for the *decR* mutant under the same

193 conditions because it has lost some ability to import and degrade cysteine. For the higher total added

194 cysteine concentrations of 1 and 2 mM, the cysteine concentration in the exposure medium decreases over

195 time, but the differences between the wild-type and *decR* mutant are not statistically significant.

Hg sorption measurements and thermodynamic calculations

197 The concentration of dissolved and cell-bound Hg was quantified in wild-type and *decR* mutant assays as

198 a function of incubation time, added cysteine, and added Hg (Figure 3). For many measurements, the

199 sums of the dissolved and cell-bound concentrations do not add to the total added Hg, which we observed

200 in our previous studies on *E. coli*.[35, 36] We interpreted this as a result of Hg(II) reduction to Hg(0),

201 potentially from outer membrane cytochromes,[47] and loss from volatilization. When the wild-type and

202 *decR* mutant were exposed to either 50 nM or 500 nM Hg without cysteine, the cell-bound Hg is between

203 50 to 65% of the total added Hg after 1 hour of exposure and does not change significantly after 3 hours

204 (Figure 3A,E,G, and K). The dissolved Hg for these conditions remains between 0 and 5% of the total

205 added Hg after 1 hour of exposure, demonstrating efficient Hg(II) sorption by cells in the absence of

206 added cysteine.

207   To understand whether conditions favored Hg(II)-sulfide or Hg(II)-cysteine species formation for

208 the experiments involving cysteine exposure in Figure 3, we calculated the Hg(II) speciation in the

209 exposure medium at each time point (Figure 4). Specifically, we present the sum of the concentrations of

210 the Hg(II)-cysteine species as well as $HgS_{(s)}$ (dissolved Hg(II)-sulfide species were negligible) as a

211 fraction of the total added Hg. Our thermodynamic calculations incorporated the total sulfide, cysteine

212 (reduced), and total recoverable Hg concentration measured in the exposure medium (e.g., information

213 from Figures 1, 2, and 3), which we also summarize in Table S3 for reference. We did not test the

214 exposure medium for other thiols secreted by the cells (e.g., glutathione). However, it is unlikely that

215 these secreted thiols would reach a concentration in the exposure medium that could influence Hg

216 speciation in the presence of 0.5 – 2 mM added cysteine. The measured total recoverable Hg was used in

217 these calculations so that the results reflect whether the conditions would favor $HgS_{(s)}$ or Hg(II)-cysteine

11

218   formation prior to Hg(II) sorption to cells. Our predictions for $HgS_{(s)}$ formation in the presence of excess

219   cysteine generally agree with the measured fraction of cell-bound Hg. For example, we predict a

220   significant amount of $HgS_{(s)}$ formation when the wild-type strain is exposed to 50 nM Hg(II) and 0.5 or 1

221   mM cysteine as well as 500 nM Hg(II) and 1 mM cysteine (Figure 4A,B,D), and we concurrently observe

222   a significant amount of cell-bound Hg (Figure 3B,C,F). In addition, when the *decR* mutant strain is

223   exposed to 50 nM Hg and 0.5 mM cysteine as well as 500 nM Hg and 1 mM cysteine, we predict a

224   majority of $HgS_{(s)}$ formation (Figure 4E,H) and observe a majority of cell-bound Hg(II) (Figure 3H,L).

225   The one exception is the 1 hour time point for the *decR* mutant exposed to 50 nM Hg and 0.5 mM

226   cysteine where $HgS_{(s)}$ is predicted to be ~50% of the total added Hg (Figure 4E), but the measured

227   fraction of cell-bound Hg(II) is <10% of the total added Hg (Figure 3H). When the majority of Hg(II) is

228   predicted to remain bound to cysteine in the exposure medium (i.e., Figure 4C,F,G), we see little cell-

229   bound Hg(II) and mostly dissolved Hg(II) (Figure 3D,I,J). Thus, there appears to be a link between

230   dissolved Hg(II) and Hg(II)-cysteine complexes outside the cell due to insufficient sulfide production to

231   shift the equilibrium to $HgS_{(s)}$ formation in the presence of excess cysteine.

232   ***ATP measurements***

233   In healthy cells, ATP concentrations are highly regulated and thus can be used as an indicator of

234   biological stress.[48] We assessed the potential toxic effects of cysteine exposure to the wild-type and *decR*

235   mutant strains by quantification of cellular ATP (Figure S1). The wild-type strain does not experience any

236   significant decrease in cellular ATP upon exposure to 50 nM Hg ± 1 and 2 mM cysteine or 500 nM Hg ±

237   1 mM cysteine for 3 hours (Figure S1A) compared to the cellular ATP concentration prior to exposure.

238   However, the *decR* mutant does observe a statistically significant 10 – 20% drop ($p < 0.05$) in cellular

239   ATP when exposed to 50 nM Hg + 1 and 2 mM cysteine as well as 500 nM Hg ± 1 mM cysteine (Figure

240   S1B). This decrease does not indicate a major change in cellular metabolism. Exposure of the *decR*

241   mutant to 1 and 2 mM cysteine without Hg causes the same observed decrease in ATP concentration (data

242   not shown), suggesting that the effect is due to cysteine alone. Interestingly, the greatest drop in cellular

243 ATP is observed when the *decR* mutant is exposed to 500 nM Hg without cysteine, where ATP levels are

244 $1.4 \pm 0.2 \times 10^{-18}$ mol per cell after a 3 hour exposure (a 36% drop).

Cell-associated Hg(II) coordination environments

246 While the detection limit restricts our ability to directly measure Hg(II) speciation in the exposure

247 medium, we are however able to directly probe the Hg(II) coordination environment in bacterial cells by

248 XAS for the conditions in this study. Specifically, Hg L_{III}-edge HR-XANES data were collected to

249 drastically improve the resolution of spectral features compared to conventional XANES.[43] The use of

250 crystal analyzers removes most, if not all, of the contribution of the background fluorescence photons, and

251 therefore, one can investigate the Hg(II) coordination environment in dilute systems (< 1 ppm).[49-52]

252 To corroborate the predictions for HgS$_{(s)}$ formation and subsequent cell-association, we analyzed

253 select samples from Figures 3 and 4 by HR-XANES: wild-type and *decR* mutant exposed to 500 nM

254 Hg(II) ± 1 mM cysteine and 50 nM Hg(II) ± 1 mM cysteine for 3 hours (Figure 5). Hg L_{III}-edge HR-

255 XANES reference spectra are presented in Figure S2. The references of Hg(II) bound to two sulfur atoms

256 (i.e., α-HgS$_{(s)}$ and Hg(cysteine)$_2$) contain a sharp, in-edge peak that represents a $2p_{3/2} \rightarrow 6s/5d$ electronic

257 transition.[51] This peak is absent in reference spectra of Hg bound to four sulfur atoms (i.e., β-HgS$_{(s)}$ and

258 Hg(cysteine)$_4$). Because the Hg(cysteine)$_2$ species at pH = 11.6 also has two coordinating nitrogen atoms

259 at 2.51 Å,[50] the in-edge peak is not as sharp as those with solely 2 sulfur atoms in the coordination sphere.

260 In addition, the HR-XANES spectra of the two bulk HgS$_{(s)}$ minerals – α-HgS$_{(s)}$ and β-HgS$_{(s)}$ – contain

261 defined peaks above the absorption edge that are lacking in the Hg(II)-thiol references. Thus, determining

262 the Hg(II)-sulfur coordination number and nature of the coordinating ligands (e.g., thiol or sulfide) can be

263 achieved with just the HR-XANES. Linear combination fit results, considering the Hg references

264 described above, are shown in red in Figures 5A,B,E,F,G. Some of the spectra are lacking best-fit curves

265 due to the absence of appropriate reference standards to explain the Hg(II) coordination environment

266 (Figure 5C,D,H). The HR-XANES of *E. coli* wild-type samples exposed to 500 nM Hg(II) ± 1 mM

267 cysteine are best fit with β-HgS$_{(s)}$ and Hg(cysteine)$_2$ references (Figures 5A,B), confirming our previous

268   results from conventional XAS techniques for exponentially-growing *E. coli*.[35, 36] Because we observe

269   cell-associated β-HgS$_{(s)}$ when 500 nM Hg is added without cysteine, it is clear that an endogenous sulfide

270   source beyond cysteine desulfhydrase exists and binds Hg(II). The aqueous Hg(cysteine)$_2$ at pH = 3

271   standard was a better fit to the spectra than the Hg(cysteine)$_2$ at pH = 11.6, suggesting that Hg(II) exists as

272   RS-Hg-SR with insignificant Hg-N bonding. This coordination environment is expected when Hg(II) is

273   bound to 2 cysteine residues in a protein, as is the case when Hg(II) is bound to MerP,[53] because the

274   amine groups do not coordinate Hg(II). The spectrum of wild-type *E. coli* exposed to 500 nM Hg(II) and

275   1 mM cysteine highly resembles the β-HgS$_{(s)}$ reference standard collected at room temperature. Manceau

276   et al. found that well-crystallized β-HgS$_{(s)}$ HR-XANES spectra measured at room temperature resemble

277   those of nanoparticulate β-HgS$_{(s)}$ measured at liquid helium temperature (∼10 K),[51] suggesting that the β-

278   HgS$_{(s)}$ associated with *E. coli* is nanoparticulate. We confirmed the presence of cell-associated HgS$_{(s)}$

279   nanoparticles (~100 nm diameter) with transmission electron microscopy (TEM) (Figure S4). The

280   absence of diffraction spots in the selected area electron diffraction (SAED) pattern implies that the β-

281   HgS$_{(s)}$ nanoparticles are amorphous (Figure S4C).[35]

282   Surprisingly, the *decR* mutant contained more β-HgS$_{(s)}$ when exposed to 500 nM Hg(II) compared

283   to the wild-type (75.6% vs. 58.7%; Figure 5A and 5E). Thus, the removal of one pathway for cysteine

284   degradation to sulfide in the cell actually increased the presence of cell-associated β-HgS$_{(s)}$. This increase

285   in β-HgS$_{(s)}$ formation could be a result of increased expression of other genes with cysteine desulfhydrase

286   ability to compensate for the loss of *decR*. Additionally, the Hg(II) species associated with the *decR*

287   mutant exposed to 500 nM Hg and 1 mM cysteine was primarily α-HgS$_{(s)}$, unlike the wild-type where

288   cell-associated Hg(II) was primarily β-HgS$_{(s)}$. We also detected the presence and phase of α-HgS$_{(s)}$ with

289   TEM and SAED (Figure S5 and Table S4). We previously observed the formation of *E. coli*-associated α-

290   HgS$_{(s)}$ exclusively when cysteine was present with Hg(II) and sulfide in the exposure medium, suggesting

291   that cysteine plays a role in determining the phase of HgS$_{(s)}$.[35] We predicted that the ratio of total sulfide

292   to total Hg(II) determines the phase of HgS$_{(s)}$ in the presence of cysteine. In this study, we confirmed this

14

293   prediction because cell-associated α-HgS$_{(s)}$ forms at a total sulfide to total recoverable Hg(II) ratio of 15

294   and β-HgS$_{(s)}$ forms at a ratio of 67, similar to the ratios that determined whether α-HgS$_{(s)}$ (10) or β-HgS$_{(s)}$

295   (100) formed in our previous study.[35] Because our TEM results also reveal that the HgS$_{(s)}$ particle

296   diameters are ≤ 100 nm, we confirm that the cell-bound Hg(II) measurements from Figures 3F,L are

297   actually depicting cell-associated Hg(II) and not just HgS$_{(s)}$ particles in solution that are trapped by the

298   200 nm pore size filter. HgS$_{(s)}$ nanoparticles are lipophilic, as determined by octanol-water partitioning

299   experiments,[54] which supports our finding that HgS$_{(s)}$ would prefer to attach to lipophilic cell surfaces.

300   Linear combination fits to the HR-XANES spectra of wild-type and *decR* mutant *E. coli* exposed

301   to 50 nM total Hg(II) ± 1 mM cysteine do not fit well with the references in this study. However, a fairly

302   good fit is achieved with the *decR* mutant exposed to 50 nM Hg(II) considering 49.7% β-HgS$_{(s)}$ and

303   50.3% Hg(cysteine)$_2$ species at pH = 11.6 (Figure 4G). The wild-type and mutant strains that were

304   exposed to 50 nM Hg(II) and 1 mM cysteine resemble the bulk β-HgS$_{(s)}$ reference standard measured at

305   room temperature, with slight differences. What is clear is that a sharp in-edge peak is absent, indicating

306   that there is not a significant amount of Hg that is linearly coordinated to 2 sulfur atoms. We provide the

307   spectrum of an aqueous Hg(cysteine)$_2$ reference at pH = 5 (Figure S3D) made at similar concentration

308   (wt/wt) as the bacterial samples with the lowest Hg content to show that the in-edge peak characteristic of

309   2-coordinate Hg-S would be clearly visible. Because the HR-XANES also do not resemble those of

310   Hg(SR)$_2$, Hg(SR)$_3$,[55] or Hg(SR)$_4$ and are lacking features above the edge characteristic of HgS$_{(s)}$

311   particles,[51] it is likely that Hg(II) exists as Hg-S clusters (i.e., analogous to Fe-S clusters or β-Hg$_x$S$_y$ less

312   than 1 nm in diameter[56]) with a coordination number of 4.

313   We also probed single gene deletion mutants of *E. coli* lacking cysteine desulfurase genes (i.e.,

314   *iscS* and *sufS*) with HR-XANES to explore the potential biogenic sulfide source that is responsible for

315   cell-associated β-HgS$_{(s)}$ formation when exogenous cysteine is not added to cells. Specifically, we tested

316   the ISC and SUF systems whose role are to assemble Fe-S clusters in *E. coli*. Hg(II) displaces Fe(II) from

317   Fe-S clusters *in vivo* in *E. coli* at micromolar Hg concentrations[57] and *in vitro* from the [4Fe-4S] cluster

15

318   of dehydratase family enzymes.[58] Thus, Fe-S clusters could be a source of sulfide for β-HgS$_{(s)}$ formation.

319   Specifically, we exposed *iscS* and *sufS* mutants to 500 nM Hg(II) for 3 hours. IscS and SufS perform the

320   same function of removing the S^0 from L-cysteine and donating it to the scaffold protein for Fe-S cluster

321   formation, but the ISC system operates under normal conditions, while the SUF system functions under

322   stress conditions.[19] From the HR-XANES spectra, the loss of the *sufS* gene had no effect on the Hg(II)

323   coordination environment for cells exposed to 500 nM Hg(II) (Figure 5A and S3A). In contrast, the linear

324   combination fit to the spectra of the *iscS* mutant exposed to 500 nM Hg(II) indicates less β-HgS$_{(s)}$

325   compared to the wild-type and *sufS* mutant. Therefore, Fe-S clusters are a likely sulfide source for β-

326   HgS$_{(s)}$ formation under normal growth conditions, although more work should be done to determine the

327   effect of *iscS* loss on cell physiology. The deletion of genes involved in cysteine degradation to sulfide for

328   Fe-S cluster formation did not eliminate HgS$_{(s)}$ formation in cell samples, likely due to the fact that only

329   single gene deletion mutants were tested. However, microbial cells are not viable after the elimination of

330   both ISC and SUF mechanisms for Fe-S cluster formation without significantly altering cell

331   metabolism.[59] In addition, another sulfide source in the cell that was not tested in this study could be

332   assimilatory sulfate reduction, which is the primary route of cysteine synthesis in bacteria like *E. coli* and

333   *Salmonella enterica* serovar Typhimurium.[27] In this pathway, which differs from dissimilatory sulfate

334   reduction by anaerobic organisms,[60] sulfate is reduced to sulfite and then sulfide via sulfite reductase.

335   Cysteine is then synthesized from sulfide and O-acetylserine with O-acetylserine (thiol)-lyase.

336   We found a striking difference in the HR-XANES spectra of the same sample (wild-type exposed

337   to 50 nM Hg + 1 mM cysteine) that was prepared by 2 different methods for HR-XANES collection. The

338   first method, which was used for all samples in this study, involved flash freezing the sample in liquid

339   nitrogen and keeping it frozen throughout the measurement. The second method involved flash-freezing

340   the sample in liquid nitrogen, freeze-drying, pressing into a pellet, and re-freezing prior to data collection

341   (compare Figure 5D and Figure S3C). We observed a similar change in Hg speciation (with XAS

342   analysis) after a flash-frozen sample thawed and then re-froze, although it was not freeze-dried.[36] The

343 freeze/thaw process may deteriorate the cell's membrane integrity, causing a change in Hg(II) speciation

344 in the cell. Freeze-drying bacteria without a cryo-protectant (e.g., 10% sucrose) will compromise

345 membrane integrity,[61] and implies that the cell-associated Hg species, at least for that particular sample, is

346 sensitive to membrane damage. Fe-S clusters exist under reducing conditions in cells, are sensitive to

347 oxygen species, and decompose upon exposure.[62] Hg-S clusters may have a similar sensitivity to oxygen

348 exposure.

349 ***Implications for Hg(II) bioavailability***

350 Early bacterial Hg(II) uptake studies suggested that neutral Hg(II)-sulfide complexes formed the

351 bioavailable fraction of Hg(II) and were transported across the cell membrane layers by passive

352 diffusion.[33, 63] More recently, evidence for energy-dependent Hg(II) biouptake has been reported, although

353 these experiments were all performed in the presence of thiols (mainly cysteine). Schaefer et al. proposed

354 that the entire Hg(II)-cysteine complex was taken up by an unknown metal-transport protein.[4] Liu et al.

355 stated that cysteine may facilitate the ligand exchange of Hg(II) with a metal transport protein responsible

356 for Hg(II) biouptake.[14]

357   We show herein that when *E. coli* is exposed to Hg(II)-cysteine complexes in the presence of

358 excess cysteine, Hg(II) will become associated with the wild-type strain but not a cysteine desulfhydrase

359 deletion mutant under otherwise the same experimental conditions and with minimal differences in cell

360 physiology (as determined by cellular ATP concentration). The main difference between the wild-type

361 and *decR* mutant assays involving added cysteine was the concentration of total sulfide in the exposure

362 medium, and calculations for Hg(II)-sulfide species formation correlate with our measurements for cell-

363 bound Hg(II). The degradation of cysteine to sulfide is an energy dependent process, which could have

364 been mistakenly recognized as an active transport mechanism for Hg(II) biouptake in the presence of

365 added cysteine in past studies. Thermodynamic calculations for $HgS_{(s)}$ formation are rather accurate in

366 predicting when Hg(II) becomes associated with the cells, indicating that the ligand exchange from

367 Hg(II)-cysteine complexes to Hg(II)-sulfides is not kinetically limited at the time scale of our experiment.

17

368   The Hg L$_{III}$-edge HR-XANES spectra never indicate that Hg(SR)$_2$ species are associated with either the

369   wild-type or *decR* mutant cells after exposure to Hg(II) in the presence of excess cysteine; the cell-

370   associated Hg(II) is either clearly HgS$_{(s)}$ or Hg-S clusters with a Hg coordination number greater than 3.

371   This suggests that ligand exchange reactions between Hg(SR)$_2$ complexes outside the cell (i.e.,

372   Hg(cysteine)$_2$) and thiols in the cell membrane are not favorable. While our evidence suggests that the

373   Hg(II) uptake pathway in the presence of excess cysteine involves a speciation change from Hg(II)-

374   cysteine complexes to Hg(II)-sulfide species and Hg-S clusters, the uptake pathway remains unknown.

375   Understanding the formation of the cell-associated Hg-S clusters observed by HR-XANES both

376   in the presence and absence of added excess cysteine could provide some insight into the Hg(II) uptake

377   mechanism. Potentially, the Hg-S clusters are analogous to Fe-S clusters in proteins and capped by

378   cysteine, which could create the HR-XANES spectra that we observe. As suggested by Manceau et al., it

379   is also possible that Fe-S clusters serve as the scaffold for HgS nucleation, leading to the formation of a

380   HgS mineral core that is functionalized by cysteine residues.[49] Depending on the total added Hg

381   concentration, the seed HgS mineral may have only a few Hg atoms, and classify as a Hg-S cluster. There

382   might also be a biological response from the ISC and SUF systems upon Hg exposure to sequester Hg(II)

383   as HgS.[64] Although we only have evidence of Hg-S cluster formation after 3 hours of exposure and no

384   localization information, it is possible that these Hg species that dominate the cell-associated Hg at the

385   lowest tested Hg concentrations are the form that undergoes biouptake.

386   Because our results suggest that Hg(II)-sulfide species formation is a critical step for bacterial

387   Hg(II) uptake in the presence of excess added cysteine, it is interesting that previous studies have shown

388   that the presence of sulfide alone (in the absence of exogenous thiols) prevents Hg(II) uptake.[4, 65] This is

389   likely due to the formation of HgS$_{(s)}$ particles that are too large to be bioavailable.[35] Graham et al.

390   suggested that the coexistence of cysteine and sulfide can promote the formation of small, disordered

391   HgS$_{(s)}$ nanoparticles that are able to passively diffuse through the cell's membrane layers.[10, 12] Our

392   previous results with STEM-EDS provided direct evidence of HgS$_{(s)}$ nanoparticles attached to the cell

18

393   surface/extracellular matrix in *E. coli* and *G. sulfurreducens* that were likely physically limited from

394   entering the cell cytoplasm.[35] Potentially, Hg(II)-sulfide complexes and/or small Hg-S clusters enter the

395   cytoplasm via passive diffusion, as suggested previously, and the size of the Hg(II)-sulfide species is an

396   important factor determining bioavailability.

Conclusion

398   The present study demonstrates that the bacterial sulfur metabolism (beyond dissimilatory sulfate

399   reduction) can have a large influence on cell-associated Hg(II) coordination and Hg(II) biouptake. We

400   show that the degradation of cysteine to sulfide and the formation of Hg(II)-sulfide species are critical for

401   the biouptake of Hg(II) in the presence of excess cysteine in the exposure medium. These results may

402   help elucidate Hg(II) bioavailability under sulfidic conditions where both sulfide and thiol groups of

403   organic matter compete to bind Hg(II) in environmental systems. Although these studies have been

404   conducted with *E. coli*, which is unable to methylate Hg(II), many diverse organisms, in addition to *E.*

405   *coli*, experience enhanced Hg(II) uptake with added cysteine, including Hg-methylators (e.g., *G.*

406   *sulfurreducens*,[4, 5] *Desulfovibrio desulfuricans*,[4] *Geobacter bemidjiensis* Bem[15]) and other non-

407   methylators (e.g., *Shewanella Oneidensis*[3]). Also, many diverse organisms are known to degrade cysteine

408   by desulfhydrase enzymes.[27, 30, 66, 67] Therefore, the findings from this study on *E. coli* likely apply to

409   organisms that are similarly affected by cysteine in their uptake of Hg(II). The role of cellular sulfur

410   metabolism, and in particular Fe-S clusters, in relation to Hg(II) biouptake should be explored further.

Conflicts of Interest

412   There are no conflicts of interest to declare.

Acknowledgements

427

428

References

430

431   1.   J. M. Parks, A. Johs, M. Podar, R. Bridou, R. A. Hurt, S. D. Smith, S. J. Tomanicek, Y. Qian, S.
432   D. Brown, C. C. Brandt, A. V. Palumbo, J. C. Smith, J. D. Wall, D. A. Elias and L. Y. Liang, The
433   genetic basis for bacterial mercury methylation, *Science*, 2013, **339**, 1332-1335.

434   2.   S. A. Chiasson-Gould, J. M. Blais and A. J. Poulain, Dissolved organic matter kinetically controls
435   mercury bioavailability to bacteria, *Environ. Sci. Technol.*, 2014, **48**, 3153-3161.

436   3.   A. Szczuka, F. M. M. Morel and J. K. Schaefer, Effect of thiols, zinc, and redox conditions on Hg
437   uptake in *Shewanella oneidensis*, *Environ. Sci. Technol.*, 2015, **49**, 7432-7438.

438   4.   J. K. Schaefer, S. S. Rocks, W. Zheng, L. Y. Liang, B. H. Gu and F. M. M. Morel, Active
439   transport, substrate specificity, and methylation of Hg(II) in anaerobic bacteria, *P.. Natl. Acad.*
440   *Sci. U.S.A.*, 2011, **108**, 8714-8719.

441   5.   J. K. Schaefer and F. M. M. Morel, High methylation rates of mercury bound to cysteine by
442   *Geobacter sulfurreducens*, *Nat. Geosci.*, 2009, **2**, 123-126.

443   6.   L. Zhao, H. Chen, X. Lu, H. Lin, G. A. Christensen, E. M. Pierce and B. Gu, Contrasting effects
444   of dissolved organic matter on mercury methylation by *Geobacter sulfurreducens* PCA and
445   *Desulfovibrio desulfuricans* ND132, *Environ. Sci. Technol.*, 2017, **51**, 10468-10475.

446   7.   H. Lin, X. Lu, L. Y. Liang and B. H. Gu, Cysteine inhibits mercury methylation by *Geobacter*
447   *sulfurreducens* PCA mutant Δ*omcBESTZ*, *Environ. Sci. Technol. Lett.*, 2015, **2**, 144-148.

448   8.   A. L. Dahl, J. Sanseverino and J. F. Gaillard, Bacterial bioreporter detects mercury in the
449   presence of excess EDTA, *Environ. Chem.*, 2011, **8**, 552-560.

450   9.   U. Ndu, T. Barkay, R. P. Mason, A. T. Schartup, R. Al-Farawati, J. Liu and J. R. Reinfelder, The
451   use of a mercury biosensor to evaluate the bioavailability of mercury-thiol complexes and
452   mechanisms of mercury uptake in bacteria, *Plos One*, 2015, **10,** e0138333.

453   10.   A. M. Graham, G. R. Aiken and C. C. Gilmour, Dissolved organic matter enhances microbial
454   mercury methylation under sulfidic conditions, *Environ. Sci. Technol.*, 2012, **46**, 2715-2723.

455   11.   S. A. Thomas, T. Z. Tong and J. F. Gaillard, Hg(II) bacterial biouptake: The role of
456   anthropogenic and biogenic ligands present in solution and spectroscopic evidence of ligand
457   exchange reactions at the cell surface, *Metallomics*, 2014, **6**, 2213-2222.

458   12.   A. M. Graham, G. R. Aiken and C. C. Gilmour, Effect of dissolved organic matter source and
459   character on microbial Hg methylation in Hg-S-DOM solutions, *Environ. Sci. Technol.*, 2013, **47**,
460   5746-5754.

461   13.   U. Skyllberg, Competition among thiols and inorganic sulfides and polysulfides for Hg and
462   MeHg in wetland soils and sediments under suboxic conditions: Illumination of controversies and
463   implications for MeHg net production, *J. Geophys. Res-Biogeo.*, 2008, **113**.

464   14.   Y. R. Liu, X. Lu, L. D. Zhao, J. An, J. Z. He, E. M. Pierce, A. Johs and B. H. Gu, Effects of
465   cellular sorption on mercury bioavailability and methylmercury production by *Desulfovibrio*
466   *desulfuricans* ND132, *Environ. Sci. Technol.,* 2016, **50**, 13335-13341.

467   15.   X. Lu, Y. R. Liu, A. Johs, L. D. Zhao, T. S. Wang, Z. M. Yang, H. Lin, D. A. Elias, E. M. Pierce,
468   L. Y. Liang, T. Barkay and B. H. Gu, Anaerobic mercury methylation and demethylation by
469   *Geobacter bemidjiensis* Bem, *Environ. Sci. Technol.*, 2016, **50**, 4366-4373.

470   16.   A. Sekowska, H. F. Kung and A. Danchin, Sulfur metabolism in *Escherichia coli* and related
471   bacteria: Facts and fiction, *J. Mol. Microb. Biotech.*, 2000, **2**, 145-177.

472   17.   N. M. Kredich, Biosynthesis of cysteine, *EcoSal Plus*, 2008, **3**.

473   18.   D. C. Johnson, D. R. Dean, A. D. Smith and M. K. Johnson, Structure, function, and formation of
474   biological iron-sulfur clusters, *Annu. Rev. Biochem.*, 2005, **74**, 247-281.

475   19.   B. Blanc, C. Gerez and S. A. de Choudens, Assembly of Fe/S proteins in bacterial systems
476   biochemistry of the bacterial ISC system, *BBA-Mol. Cell Res.,* 2015, **1853**, 1436-1447.

477   20.   Y. Bai, T. Chen, T. Happe, Y. Lu and A. Sawyer, Iron-sulphur cluster biogenesis via the SUF
478   pathway, *Metallomics*, 2018, **10**.

479   21.   E. L. Mettert and P. J. Kiley, How is Fe-S cluster formation regulated?, *Annu. Rev. Microbiol.,*
480   2015, **69**, 505-526.

481   22.   B. Roche, L. Aussel, B. Ezraty, P. Mandin, B. Py and F. Barras, Iron/sulfur proteins biogenesis in
482   prokaryotes: Formation, regulation and diversity, *BBA-Bioenergetics*, 2013, **1827**, 455-469.

483   23.   S. J. Lippard and J. M. Berg, *Principles of bioinorganic chemistry*, University Science Books,
484   Mill Valley, CA, 1994.

485 24. E. Guédon and I. Martin-Verstraete, in *Amino acid biosynthesis - pathways, regulation, and*
486   *metabolic engineering*, ed. V. F. Wendisch, Springer Berlin Heidelberg, Berlin, Heidelberg, 2007,
487   pp. 195-218.

488 25. N. Awano, M. Wada, H. Mori, S. Nakamori and H. Takagi, Identification and functional analysis
489   of *Escherichia coli* cysteine desulfhydrases, *Appl. Environ. Microbiol.*, 2005, **71**, 4149-4152.

490 26. N. Awano, M. Wada, A. Kohdoh, T. Oikawa, H. Takagi and S. Nakamori, Effect of cysteine
491   desulfhydrase gene disruption on L-cysteine overproduction in *Escherichia coli*, *Appl. Microbiol.*
492   *Biot.*, 2003, **62**, 239-243.

493 27. T. Oguri, B. Schneider and L. Reitzer, Cysteine catabolism and cysteine desulfhydrase
494   (CdsH/STM0458) in *Salmonella enterica* serovar Typhimurium, *J. Bacteriol.*, 2012, **194**, 4366-
495   4376.

496 28. T. Shimada, K. Tanaka and A. Ishihama, Transcription factor DecR (YbaO) controls
497   detoxification of L-cysteine in *Escherichia coli*, *Microbiol-Sgm*, 2016, **162**, 1698-1707.

498 29. S. I. Tchong, H. M. Xu and R. H. White, L-cysteine desulfidase: An [4Fe-4S] enzyme isolated
499   from *Methanocaldococcus jannaschii* that catalyzes the breakdown of L-cysteine into pyruvate,
500   ammonia, and sulfide, *Biochemistry-Us*, 2005, **44**, 1659-1670.

501 30. K. Takumi and G. Nonaka, Bacterial cysteine-inducible cysteine resistance systems, *J Bacteriol*,
502   2016, **198**, 1384-1392.

503 31. A. K. Bachhawat and A. Kaur, Glutathione degradation, *Antioxid. Redox. Sign.*, 2017, **27**, 1200-
504   1216.

505 32. H. Suzuki, S. Kamatani, E.-S. Kim and H. Kumagai, Aminopeptidases A, B, and N and
506   dipeptidase D are the four cysteinylglycinases of *Escherichia coli* K-12, *J. Bacteriol.*, 2001, **183**,
507   1489.

508 33. J. M. Benoit, C. C. Gilmour and R. P. Mason, Aspects of bioavailability of mercury for
509   methylation in pure cultures of *Desulfobulbus propionicus* (1pr3), *Appl. Environ. Microbiol.*,
510   2001, **67**, 51-58.

511 34. A. Drott, L. Lambertsson, E. Björn and U. Skyllberg, Importance of dissolved neutral mercury
512   sulfides for methyl mercury production in contaminated sediments, *Environ. Sci. Technol.*, 2007,
513   **41**, 2270-2276.

514 35. S. A. Thomas, K. E. Rodby, E. W. Roth, J. Wu and J.-F. Gaillard, Spectroscopic and microscopic
515   evidence of biomediated hgs species formation from Hg(II)–cysteine complexes: Implications for
516   Hg(II) bioavailability, *Environ. Sci. Technol.*, 2018, **52**, 10030-10039.

517 36. S. A. Thomas and J.-F. Gaillard, Cysteine addition promotes sulfide production and 4-fold
518   Hg(II)–S coordination in actively metabolizing *Escherichia coli, Environ. Sci. Technol.*, 2017, **51**,
519   4642-4651.

520 37. T. Baba, T. Ara, M. Hasegawa, Y. Takai, Y. Okumura, M. Baba, K. A. Datsenko, M. Tomita, B.
521   L. Wanner and H. Mori, Construction of Escherichia coli K-12 in-frame, single-gene knockout
522   mutants: The Keio collection, *Mol. Syst. Biol.*, 2006, **2** 2006.0008.

523 38. C. Ranquet, S. Ollagnier-de-Choudens, L. Loiseau, F. Barras and M. Fontecave, Cobalt stress in
524   *Escherichia coli* - the effect on the iron-sulfur proteins, *J. Biol. Chem.*, 2007, **282**, 30442-30451.

525 39. J. D. Cline, Spectrophotometric determination of hydrogen sulfide in natural waters, *Limnol.*
526   *Oceanogr.*, 1969, **14**, 454-&.

527 40. P. Nagy, Z. Palinkas, A. Nagy, B. Budai, I. Toth and A. Vasas, Chemical aspects of hydrogen
528   sulfide measurements in physiological samples, *BBA-Gen. Subjects*, 2014, **1840**, 876-891.

529 41. M. K. Gaitonde, A spectrophotometric method for direct determination of cysteine in presence of
530   other naturally occurring amino acids, *Biochem. J.*, 1967, **104**, 627-633.

531 42. B. Mishra, E. J. O'Loughlin, M. I. Boyanov and K. M. Kemner, Binding of Hg-II to high-affinity
532   sites on bacteria inhibits reduction to Hg-0 by mixed Fe-II/III phases, *Environ. Sci. Technol.,*
533   2011, **45**, 9597-9603.

534 43. O. Proux, E. Lahera, W. Del Net, I. Kieffer, M. Rovezzi, D. Testemale, M. Irar, S. Thomas, A.
535   Aguilar-Tapia, E. F. Bazarkina, A. Prat, M. Tella, M. Auffan, J. Rose and J.-L. Hazemann, High-
536   energy resolution fluorescence detected X-ray absorption spectroscopy: A powerful new
537   structural tool in environmental biogeochemistry sciences, *J. Environ. Qual.*, 2017, **46**, 1146-
538   1157.

539 44. B. Ravel and M. Newville, Athena, Artemis, Hephaestus: Data analysis for X-ray absorption
540   spectroscopy using IFEFFIT, *J. Synchrotron Radiat.*, 2005, **12**, 537-541.

541 45. http://www.eawag.ch/en/department/surf/projects/chemeql/ (accessed Nov. 12, 2016).

542 46. G. Nonaka and K. Takumi, Cysteine degradation gene *yhaM*, encoding cysteine desulfidase,
543   serves as a genetic engineering target to improve cysteine production in *Escherichia coli*, *Amb.*
544   *Express*, 2017, **7**, 90.

545 47. H. Y. Hu, H. Lin, W. Zheng, B. Rao, X. B. Feng, L. Y. Liang, D. A. Elias and B. H. Gu, Mercury
546   reduction and cell-surface adsorption by *Geobacter sulfurreducens* PCA, *Environ. Sci. Technol.*,
547   2013, **47**, 10922-10930.

548 48. S. P. M. Crouch, R. Kozlowski, K. J. Slater and J. Fletcher, The use of ATP bioluminescence as a
549   measure of cell-proliferation and cytotoxicity, *J. Immunol. Methods*, 1993, **160**, 81-88.

550 49. A. Manceau, J. X. Wang, M. Rovezzi, P. Glatzel and X. B. Feng, Biogenesis of mercury-sulfur
551   nanoparticles in plant leaves from atmospheric gaseous mercury, *Environ. Sci. Technol.,* 2018,
552   **52**, 3935-3948.

553 50. A. Manceau, M. Enescu, A. Simionovici, M. Lanson, M. Gonzalez-Rey, M. Rovezzi, R.
554   Tucoulou, P. Glatzel, K. L. Nagy and J. P. Bourdineaud, Chemical forms of mercury in human
555   hair reveal sources of exposure, *Environ. Sci. Technol.*, 2016, **50**, 10721-10729.

556 51. A. Manceau, C. Lemouchi, M. Enescu, A. C. Gaillot, M. Lanson, V. Magnin, P. Glatzel, B. A.
557   Poulin, J. N. Ryan, G. R. Aiken, I. Gautier-Luneau and K. L. Nagy, Formation of mercury sulfide
558   from Hg(II)-thiolate complexes in natural organic matter, *Environ. Sci. Technol.*, 2015, **49**, 9787-
559   9796.

1
2
3
4
5
6
7
8
9
10
11
12
13
14
15
16
17
18
19
20
21
22
23
24
25
26
27
28
29
30
31
32
33
34
35
36
37
38
39
40
41
42
43
44
45
46
47
48
49
50
51
52
53
54
55
56
57
58
59
60

23

560   52.   A. Manceau, M. Merkulova, M. Murdzek, V. Batanova, R. Baran, P. Glatzel, B. K. Saikia, D.
561   Paktunc and L. Lefticariu, Chemical forms of mercury in pyrite: Implications for predicting
562   mercury releases in acid mine drainage settings, *Environ. Sci. Technol.*, 2018, **52,** 10286-10296.

563   53.   R. A. Steele and S. J. Opella, Structures of the reduced and mercury-bound forms of MerP, the
564   periplasmic protein from the bacterial mercury detoxification system, *Biochemistry-Us*, 1997, **36**,
565   6885-6895.

566   54.   A. Deonarine and H. Hsu-Kim, Precipitation of mercuric sulfide nanoparticles in NOM-
567   containing water: Implications for the natural environment, *Environ. Sci. Technol.*, 2009, **43**,
568   2368-2373.

569   55.   A. Manceau, C. Lemouchi, M. Rovezzi, M. Lanson, P. Gatzel, K. L. Nagy, I. Gautier-Luneau, Y.
570   Joly and M. Enescu, Structure, bonding, and stability of mercury complexes with thiolate and
571   thioether ligands from high-resolution XANES spectroscopy and first-principles calculations,
572   *Inorg. Chem.*, 2015, **54**, 11776-11791.

573   56.   J.-P. Bourdineaud, M. Gonzalez-Rey, M. Rovezzi, P. Glatzel, K. L. Nagy and A. Manceau,
574   Divalent mercury in dissolved organic matter is bioavailable to fish and accumulates as dithiolate
575   and tetrathiolate complexes, *Environ. Sci. Technol.,* 2019, **53**, 4880-4891.

576   57.   S. P. LaVoie, D. T. Mapolelo, D. M. Cowart, B. J. Polacco, M. K. Johnson, R. A. Scott, S. M.
577   Miller and A. O. Summers, Organic and inorganic mercurials have distinct effects on cellular
578   thiols, metal homeostasis, and Fe-binding proteins in *Escherichia coli*, *J. Biol. Inorg. Chem.*,
579   2015, **20**, 1239-1251.

580   58.   F. F. Xu and J. A. Imlay, Silver(I), mercury(II), cadmium(II), and zinc(II) target exposed enzymic
581   iron-sulfur clusters when they toxify *Escherichia coli*, *Appl. Environ. Microbiol.*, 2012, **78**, 3614-
582   3621.

583   59.   N. Tanaka, M. Kanazawa, K. Tonosaki, N. Yokoyama, T. Kuzuyama and Y. Takahashi, Novel
584   features of the ISC machinery revealed by characterization of *Escherichia coli* mutants that
585   survive without iron–sulfur clusters, *Mol. Microbiol.*, 2015, **99**, 835-848.

586   60.   N. Pfennig, F. Widdel and H. G. Trüper, in *The prokaryotes: A handbook on habitats, isolation,*
587   *and identification of bacteria*, eds. M. P. Starr, H. Stolp, H. G. Trüper, A. Balows and H. G.
588   Schlegel, Springer Berlin Heidelberg, Berlin, Heidelberg, 1981, pp. 926-940.

589   61.   P. Wessman, S. Hakansson, K. Leifer and S. Rubino, Formulations for freeze-drying of bacteria
590   and their influence on cell survival, *Jove-J. Vis. Exp.*, 2013, DOI: UNSP e4058

591   10.3791/4058.

592   62.   J. A. Imlay, Iron-sulphur clusters and the problem with oxygen, *Mol. Microbiol.*, 2006, **59**, 1073-
593   1082.

594   63.   J. M. Benoit, C. C. Gilmour, R. P. Mason and A. Heyes, Sulfide controls on mercury speciation
595   and bioavailability to methylating bacteria in sediment pore waters, *Environ. Sci. Technol.*, 1999,
596   **33**, 951–957.

597   64.   S. P. LaVoie and A. O. Summers, Transcriptional responses of *Escherichia coli* during recovery
598   from inorganic or organic mercury exposure, *BMC Genomics*, 2018, **19**, 52.

599　65.　T. Zhang, B. Kim, C. Leyard, B. C. Reinsch, G. V. Lowry, M. A. Deshusses and H. Hsu-Kim,
600　　　　Methylation of mercury by bacteria exposed to dissolved, nanoparticulate, and microparticulate
601　　　　mercuric sulfides, *Environ. Sci. Technol.*, 2012, **46**, 6950-6958.

602　66.　C. W. Forsberg, Sulfide production from cysteine by *Desulfovibrio-desulfuricans*, *Appl. Environ.*
603　　　　*Microbiol.*, 1980, **39**, 453-455.

604　67.　A. M. Graham, A. L. Bullock, A. C. Maizel, D. A. Elias and C. C. Gilmour, Detailed assessment
605　　　　of the kinetics of Hg-cell association, Hg methylation, and methylmercury degradation in several
606　　　　*Desulfovibrio* species, *Appl. Environ. Microbiol.*, 2012, **78**, 7337-7346.

607

608

609

610

611

612

613

614

615　**Figures**
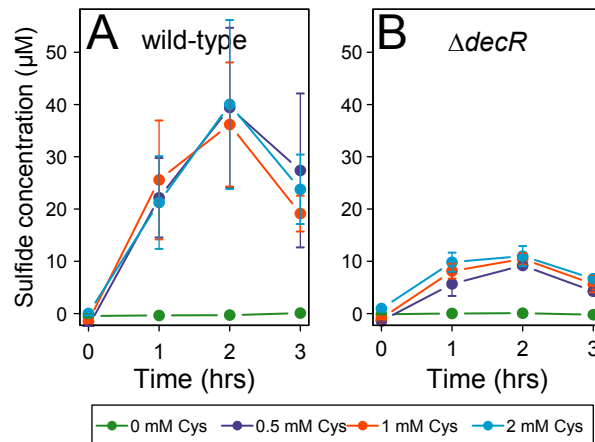
Figure 1: The concentration of sulfide in the exposure medium detected after 3-hour exposures of
(A) wild-type and (B) *decR* mutant strains of *E. coli* to 0, 0.5, 1, and 2 mM cysteine (Cys). The
points are averages from 3 independent experiments and the error bars are ± 1 S.D.

616

617

618

25

1
2
3
4
5
6
7
8
9
10
11
12
13
14
15
16
17
18
19
20
21
22
23
24
25
26
27
28
29
30
31
32
33
34
35
36
37
38
39
40
41
42
43
44
45
46
47
48
49
50
51
52
53
54
55
56
57
58
59
60

619
620
621
622
623
624
625
626
627
628
629
630
631
632
633
634
635
636
637
638
639
640
641
642
643
644
645
646
647
648
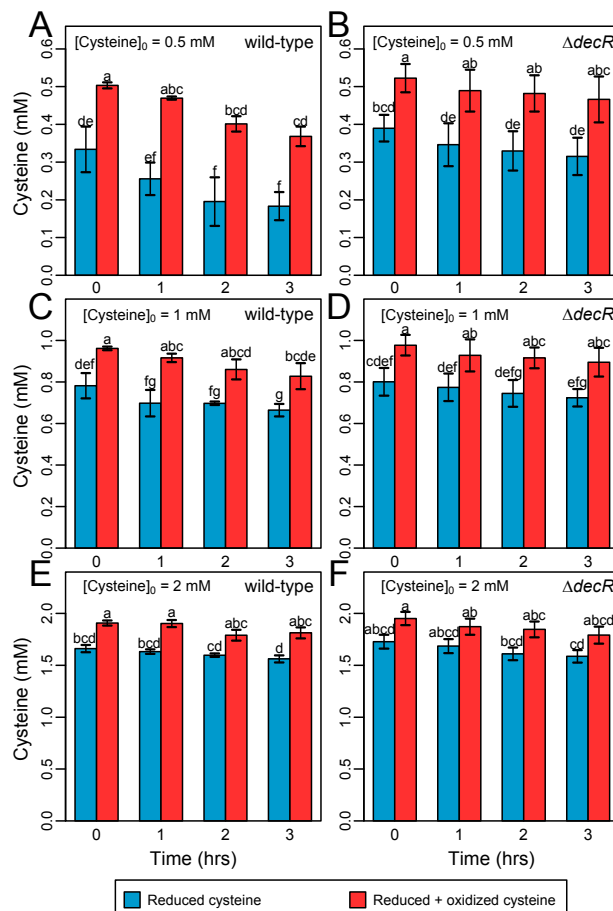
Figure 2: The concentration of reduced and reduced + oxidized cysteine (cystine) detected in the exposure medium at time = 0, 1, 2, and 3 hours during exposure of (A,C,E) wild-type and (B,D,F) *decR* mutant strains of *E. coli* to (A,B) 0.5 mM, (C,D) 1 mM, and (E,F) 2mM cysteine. Results of a Tukey's honest significant differences test are provided separately for each lettered plot. The bars are averages from 3 independent experiments and the error bars are ± 1 S.D.

26
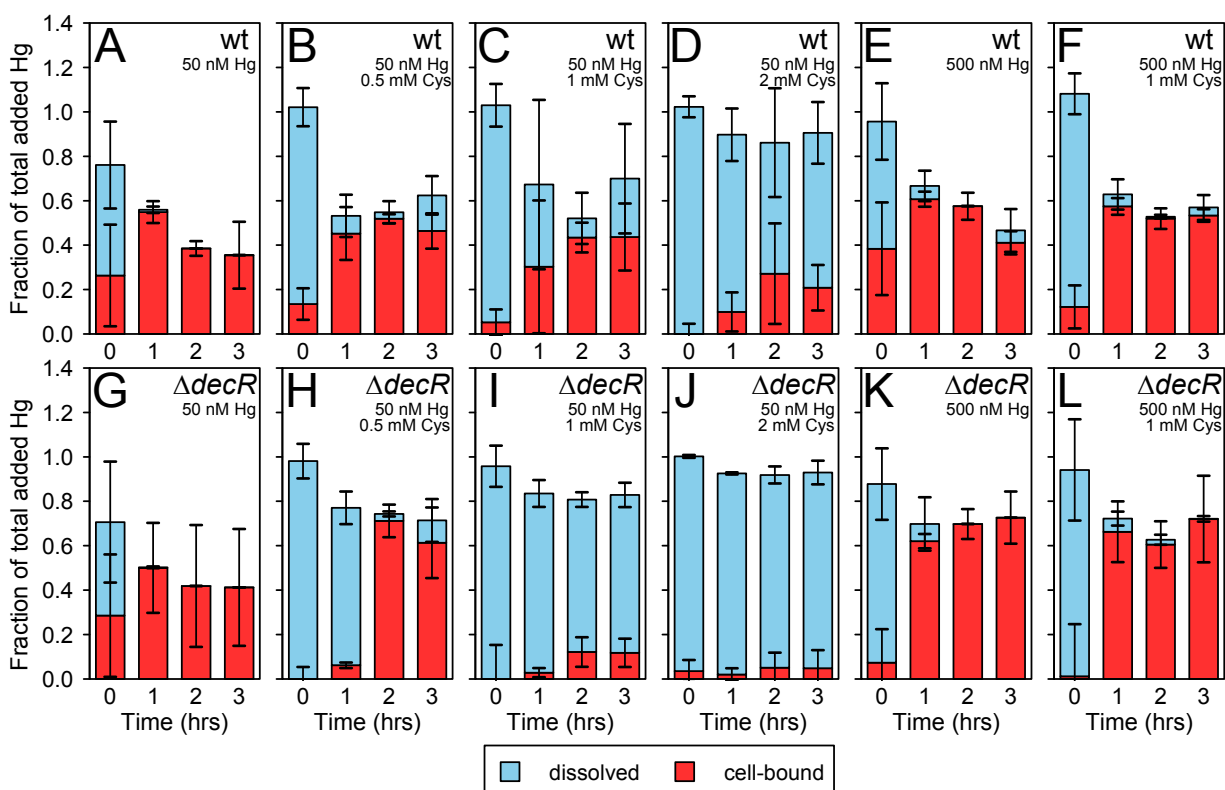
Figure 3: The dissolved and cell-bound Hg presented as a fraction of the total added Hg (i.e., 50 or 500 nM) detected after 0 to 3 hours of exposure of the (A - F) wild-type (wt) and (G - L) *decR* mutant to 50 or 500 nM total Hg. The added Hg was pre-equilibrated with either (A, E, G, K) 0 mM cysteine (Cys), (B, H) 0.5 mM Cys, (C, F, I, L) 1 mM Cys, or (D, J) 2 mM Cys. In many cases, the sum of the dissolved and cell-bound bars does not add to the total added Hg likely due to loss from Hg(II) reduction to Hg(0) and volatilization. The bars are averages from 2-3 independent experiments and the error bars are ± 1 S.D.
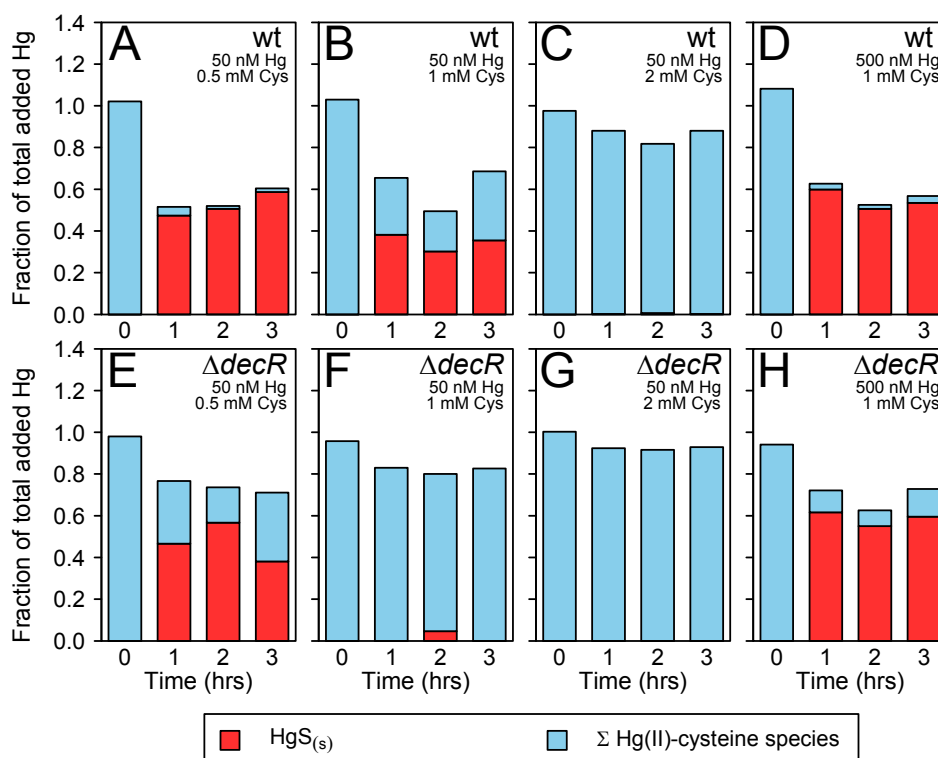
Figure 4: The predicted fraction of HgS$_{(s)}$ and Hg(II)-cysteine species that would form from the total sulfide, total cysteine, and total recoverable Hg (dissolved + cell bound) measured at each time point in the (A,B,C,D) wild-type (wt) and (E,F,G,H) *decR* mutant assays that involved cysteine exposure. The calculations are based on the thermodynamic model presented in Table S2. The total recoverable Hg was utilized in order to predict whether HgS$_{(s)}$ or Hg(II)-cysteine species formation would be favorable in the absence of cells. The results are presented as a fraction of the total added Hg (i.e., 50 or 500 nM) to be directly comparable with Figure 3.
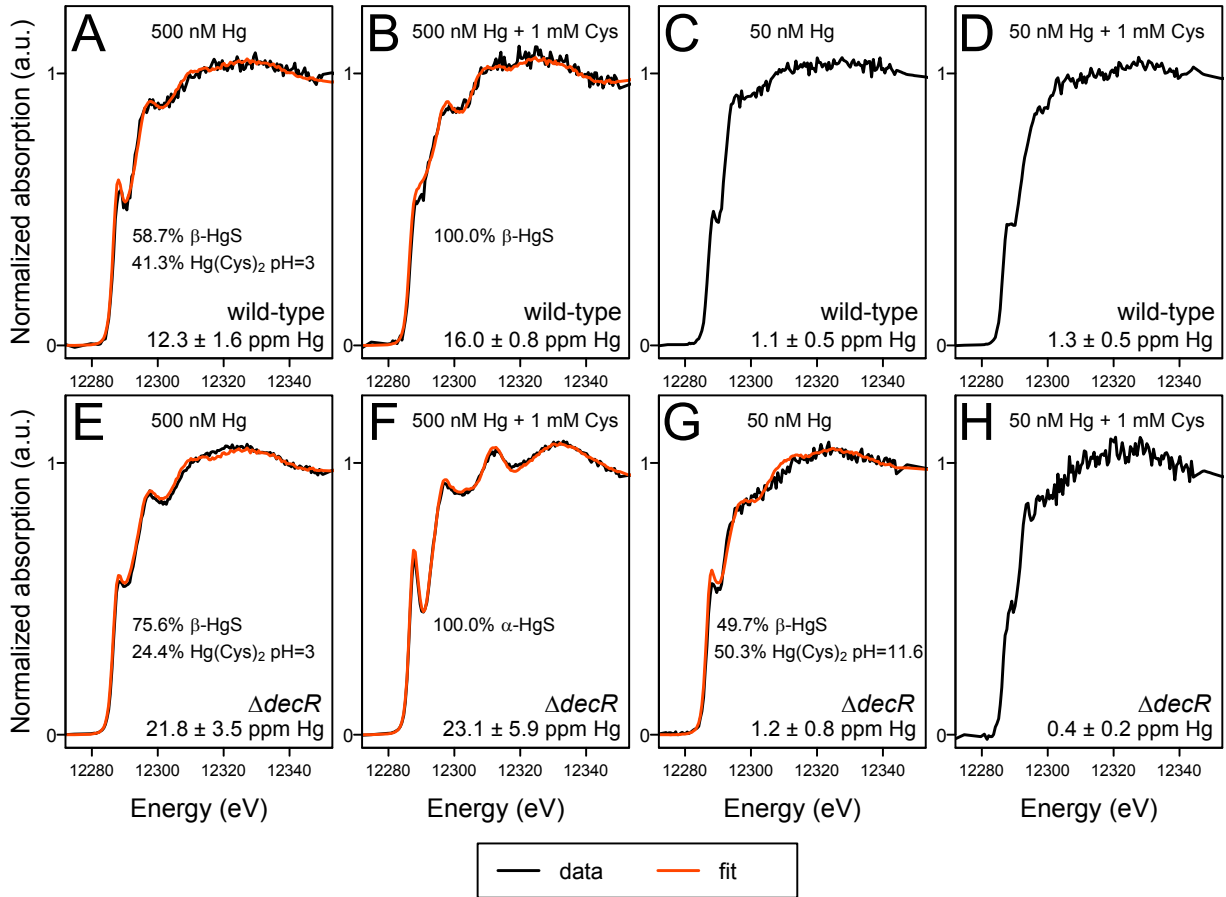
Figure 5: Hg L$_{III}$-edge HR-XANES of cell pellets of (A,B,C,D) wild-type and (E,F,G,H) *decR* mutant strains of *E. coli* that were initially exposed to 50 and 500 nM Hg with and without cysteine for 3 hours. The red line is the best-fit result of a linear combination fit, which included β-HgS, α-HgS, Hg(Cys)$_{2(aq)}$ at pH=3, and Hg(Cys)$_{2(aq)}$ at pH=11.6 as references. The spectra in plots C, D, and H are missing a best-fit result due to the absence of a reference spectrum that fits well; however, the spectra in plots C, D, and H do not contain prominent in-edge peaks that signify Hg coordination to 2 sulfur atoms. The concentration of cell-associated Hg (ppm) for each spectrum is included at the bottom of each plot.